JOURNAL OF AGRICULTURAL AND FOOD CHEMISTRY

Bruise Detection in Pacific Pink Salmon (*Oncorhynchus gorbuscha*) by Visible and Short-Wavelength Near-Infrared (SW-NIR) Spectroscopy (600−1100 nm)

MENGSHI LIN,*,† ANNA G. CAVINATO,‡ DAVID M. MAYES,§ SCOTT SMILEY,#
YIQUN HUANG,† MURAD AL-HOLY,† AND BARBARA A. RASCO†

Department of Food Science and Human Nutrition, Box 646376, Washington State University, Pullman, Washington 99164-6373; Chemistry Program, Eastern Oregon University, One University Boulevard, La Grande, Oregon 97850; D-Squared Development, 905 M Avenue, La Grande, Oregon 97850; and Fishery Industrial Technology Center, 118 Trident Way, Kodiak, Alaska 99615-7401

Visible and short-wavelength near-infrared (SW-NIR) spectroscopy (600−1100 nm) was used to detect bruises in intact, whole Pacific pink salmon (*Oncorhynchus gorbuscha*). The measurements were performed noninvasively through the skin and scales in the diffuse reflectance mode. Digital images of bruised and nonbruised regions of fish were captured after the fish samples were filleted. Image analysis was conducted using Adobe Photoshop 7.0 with relative gray values used as reference values in a partial least-squares (PLS) model. A PLS cross-validation model using six latent variables yielded a standard error of prediction (SEP = 0.05%, $R = 0.83$). Approximately 84% of all nonbruised spectra were correctly classified, whereas approximately 81% of all bruised spectra were correctly classified. These results suggest that visible and SW-NIR could be used to control the bruise defect of fish products during processing, thereby improving product consistency and quality.

KEYWORDS: Bruise; pink salmon; relative gray value; PLS; visible and SW-NIR

INTRODUCTION

There has been rapid growth over the past decade in the development and use of noninvasive methods for detecting quality defects in foods (*1*, *2*). In particular, visible and short-wavelength near-infrared (SW-NIR) spectroscopy (600−1100 nm) finds wide application in the food industry (*3*, *4*). Although examples of NIR for detecting bruises and internal defects in fruits and vegetables have been reported (*5*), evaluation of this technology for detecting quality defects in animal products, particularly in whole animals, is still limited.

Bruising is a particular problem with aquatic food products. Deep bruising is a condition that cannot be readily detected by examining the surface features of the fish. It results from pooled blood along the axial skeleton and in adjacent muscle tissue and can only be detected when the fish are filleted. Deep bruising is generally caused by crushing or injuring a fish while it is still alive by overloading a seine net, brailer bag, fish hold, or refrigerated seawater (RSW) tank.

A major challenge for fish processors in Alaska is how to evaluate the internal conditions for the fish and predict which may be bruised. Bruising is a major product defect in whole wild-caught salmon. Bruising dramatically reduces the value of fish fillets and is becoming an impediment to the sale of Alaskan-harvested salmon on the world market, particularly chum salmon. Fish are graded before they are filleted. A grade-1 quality fish when caught should be free from defects such as punctures, bites, and open scars or cuts, and no visible bruises or dark blood discoloration is allowed. For grade-2 quality fish, no more than one visible bruise (up to 6 cm^2) is permitted (*6*). Recurrent problems with Pacific salmon quality have led to a loss of market share and price for the 2003 harvest season that are among the lowest in 30 years. The deep recession in Japan and other Asian export markets has aggravated this situation. However, markets can be improved if consistent high-quality product can be ensured. Using noninvasive grading methods based on visible and SW-NIR could help solve this problem.

Visible and SW-NIR spectroscopy (600−1100 nm) has several advantages as a nondestructive method. It allows the user to collect full spectra in less than a few seconds and to analyze food samples remotely using fiber optic probes. In this wavelength range, light radiation travels over long path lengths and penetrates fish skin and scales into the muscle tissue, thus permitting analysis of intact whole fish, fish fillets or steaks, and bulk samples of roe (*7*−*11*). Visible and SW-NIR can penetrate up to 10 mm into fish muscle tissue, indicating that the penetration depth is adequate for detecting intramuscular bruises (*12*).

* Author to whom correspondence should be addressed [telephone (509) 335-7778; fax (509) 335-4815; e-mail linmengshi2001@yahoo.com].
† Washington State University.
‡ Eastern Oregon University.
§ D-Squared Development.
# Fishery Industrial Technology Center.

10.1021/jf0346197 CCC: $25.00
Published on Web 09/26/2003

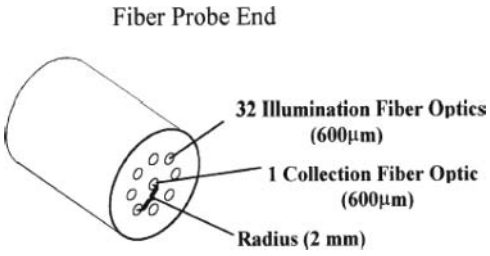

Figure 1. Fiber optic probe of DPA20 spectroscopy used to acquire spectra.

Although the use of visible and SW-NIR to detect bruises in fish muscle tissues has not been reported in the literature, several similar applications have been studied. For example, visible and SW-NIR has been used successfully to determine cerebral swelling after traumatic head injury in children, blood flow in liver tissue, and oxygenation in the cerebrum as a result of head trauma or brain injury (*13*). This line of research indicates that the pooling of blood and blood flow can be detected by visible and SW-NIR, making it a feasible technology for studying the presence of bruises in fish muscle.

Because hemoglobin and deoxyhemoglobin have strong absorbance bands in the visible and SW-NIR region (*13*), the vascularization of the gill region can be easily differentiated from muscle tissue. Visible and SW-NIR can detect the presence of muscle bruises in salmon because hemoglobin in fish muscle absorbs in this spectral region. In the visible and SW-NIR region, oxygenated hemoglobin has a broad absorption band between 600 and 1000 nm, whereas deoxygenated hemoglobin has a more prominent absorption band at ~760 nm (*13*).

Although ultrasound has been used to detect blood congestion in salmon as a means of predicting smoked salmon quality, simple diagnostic ultrasound is not useful for detecting muscle bruising in intact Pacific salmon (*14*).

The objective of this study was to evaluate the ability of visible and SW-NIR (600−1100 nm) spectroscopy to detect bruises in intact Pacific pink salmon (*Oncorhynchus gorbuscha*) by partial least-squares (PLS) modeling. The mean relative gray values (RGVs) measured on the internal surface of fish fillets by digital photography were used as reference values in the PLS modeling.

MATERIALS AND METHODS

Sample Preparation. Nine pink salmon (length = 50−65 cm) were harvested off the coast of Kodiak, AK, during the 2001 commercial opening. Immediately upon capture, fish were treated to generate bruises similar to what would be expected during abusive commercial handling. The intent was to create bruising in anterior and posterior dorsal regions, along the spinal column, and near the tail.

Spectra Collection. SW-NIR spectra of whole, intact, bruised, and nonbruised pink salmon were acquired using a DPA-20 spectrophotometer (D-Squared Development, Inc., La Grande, OR). Spectra were collected with a fiber optic probe in the diffuse reflectance mode over a wavelength range from 600 to 1100 nm at 0.5 nm intervals (**Figure 1**). The probe contained 32 illumination fibers (600 μm in diameter) arranged in concentric circles 2 mm away from a central pickup fiber. Light from the internal tungsten bulb provided illumination. During the measurement, the probe was put on the lateral line of fish, starting at 1 cm from the tail fork and at ~2 cm intervals along the length of the fish. Spectra were collected on both sides of the fish. Over 20 sampling locations were selected per fish, yielding a total of 360 spectra. Before spectra were measured on the sample, dark and reference spectra were obtained with the average of 100 scans and 100 ms exposure time. Individual spectra were the average of 100 scans with 200 ms of exposure time for each sample.

Capturing Digital Images. After spectral acquisition, each fish was filleted. Fillets were placed along a ruler. The locations of bruises in the filleted fish were verified, and their positions with reference to the ruler were recorded. A digital image of the internal surface of each fish was acquired by a digital camera (Nikon, Coolpix 950) in one go, and the corresponding locations for the spectral scans were noted.

Image Analysis. Image analysis was conducted using Adobe Photoshop 7.0 software (Adobe Systems Inc., San Jose, CA). To keep the background of all images consistent, the background luminosity of each picture was adjusted and balanced to 225 ± 3. The bright dots in each image were trimmed by covering them with surrounding color.

A square image (50 × 50 pixels) corresponding to the position of the spectral measurement was cut from the digital image. The color images (in RGB mode) were converted to the gray mode. Although RGB is a standard color mode, using the red, green, or blue value individually as a reference value for the PLS modeling in this study will lead to a loss of information and yield poor prediction results. However, using the gray value, which is the average of the sum of the red, green, and blue values, will solve this problem and greatly improve the prediction accuracy in the PLS modeling. Every pixel of a gray scale image has a brightness value ranging from 0 (black) to 255 (white). The mean RGV is the ratio of the gray value to 255, with a range from 0 to 1. The mean RGV of each 50 × 50 pixel image was used as a reference value for the corresponding spectra to establish a PLS model.

Data Analysis. Data analysis was performed using Delight version 3.2.1 software (Textron Systems, Wilmington, MA). Because spectral features in visible and SW-NIR are quite overlapped, data preprocessing algorithms such as binning, smoothing, and the second-derivative transformation and multivariate statistical analysis techniques were employed to analyze the data (*7*, *8*). Binning reduces the number of data points in a spectrum by averaging n points into one. Smoothing eliminates high-frequency instrument noise by averaging neighboring data points. First, spectral data were binned by 2 nm and smoothed with a Gaussian function over 12 nm. Then a second-derivative transformation with a 12 nm gap was calculated to separate overlapping absorption bands and remove baseline offsets.

For this study, PLS calibration methods were developed. PLS methods utilize the entire spectrum in a calibration model. Leave-one-out cross-validation was used to evaluate the quality of the model (*7*, *8*). In this technique, all but one sample was used to build a calibration model and then the model was used to predict the remaining sample. Thereafter, a second sample is left out from all samples and a newly constructed model was used to predict the sample. This procedure was repeated until each sample was left out and predicted by a model once. The predicted values were then compared with the reference values. The standard error of prediction (SEP) was used to indicate the predictive performance of the calibration models:

$$\mathrm{SEP} = \sqrt{\frac{\sum_{i=1}^{n}(X - Y)^2}{n - 1}}$$

X = NIR method value, Y = reference method value, and n = the number of samples.

RESULTS AND DISCUSSION

Typical spectra recorded on bruised and nonbruised locations of Pacific pink salmon are shown in **Figure 2**. For some spectra, a prominent deoxygenated hemoglobin absorbance peak at 760 nm (*13*) is clearly observed. The amplitude of the hemoglobin absorbance in the region of a bruise was generally much higher than at other locations on the same fish or at the same location on different fish. These spectra were recorded from highly bruised locations of pink salmon muscle. However, for most other spectra recorded on nonbruised locations or slightly bruised locations, the deoxygenated hemoglobin absorbance peak is

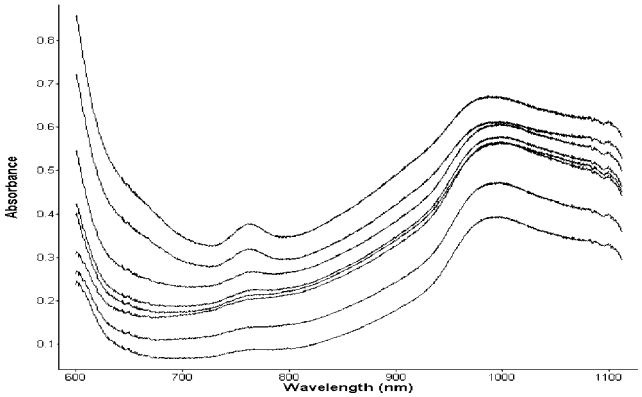

Figure 2. Typical visible and SW-NIR spectra of bruised and nonbruised locations in pink salmon muscle.

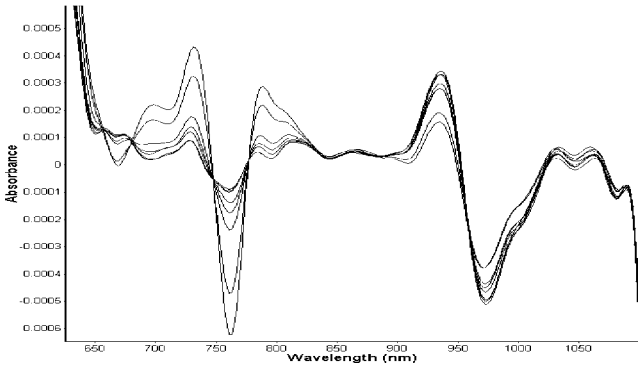

Figure 3. Second-derivative spectra (12 nm gap) of bruised and nonbruised locations in pink salmon muscle.

barely seen. Representative second-derivative spectra of bruised and nonbruised locations in pink salmon muscle are shown in **Figure 3**. The second-derivative technique is often used to process NIR data. It helps to separate overlapping absorption bands, remove baseline shifts, and increase apparent spectral resolution. This indicates that it may be possible to detect changes in the concentration of deoxygenated hemoglobin at the location of a bruise.

Hemoglobin is the primary pigment of blood. It consists of four myoglobins linked together as a tetramer. Oxyhemoglobin is bright red in color. Loss of molecular oxygen at the sixth ligand yields deoxyhemoglobin, and the color of the tissue changes to the customary purplish red. The discoloration of salmon flesh may be due to blood congestion caused by crushing and injuring, leading to competition from active mitochondria with oxyhemoglobin for oxygen, which reduces oxyhemoglobin and increases deoxyhemoglobin (*17*). In summary, the transition of oxyhemoglobin to deoxyhemoglobin contributes mainly to the bruising of salmon flesh.

Figure 4 shows four typical different degrees of bruising (heavily, moderately, and slightly bruised and nonbruised) in pink salmon muscle and black and white references (50 × 50 pixels, RGB mode). The severity of bruising is proportional to the concentration of deoxyhemoglobin (purplish red) in muscle tissue. The higher the concentration of deoxyhemoglobin, the darker the muscle tissue looks. Therefore, images become darker and darker with increased severity of bruising. Six digital images (50 × 50 pixels) of **Figure 4** were converted into the gray mode by using Adobe Photoshop 7.0, yielding six mean RGV, respectively (**Figure 5**). Using this image analysis, quantitative values for bruising can be assigned and different degrees of bruise can be differentiated. The RGVs for bruising provided reference values for corresponding spectra in a chemometric model for predicting the degrees and the absence of bruises directly from visible and SW-NIR spectral measurements.

A PLS calibration model was established for pink salmon using these data. Choosing the optimal number of latent variables is very important in PLS methods. If the model is constructed with too few latent variables, it will be inaccurate because not all of the relevant information is used. In contrast, too many latent variables will decrease the prediction accuracy as a result of overfitting (*15*). **Figure 6** shows the SEP of predictive models for bruising using different numbers of latent variables. The SEP decreases sharply and reaches the first local minimum with the first four latent variables. Then the SEP reaches a second local minimum at six latent variables. Cross-validation results (**Figure 7**) for predicting RGVs of the PLS model with four latent variables yield a coefficient of correlation ($R = 0.75$) and an SEP of 0.06%, whereas cross-validation results (**Figure 8**) of the PLS model with six latent variables yield an R of 0.83 and an SEP of 0.05%. Although use of the first local minimum for determining the optimal number of latent variables is standard practice, in this case, the PLS model with six latent variables greatly improved the R value compared with the PLS model with four latent variables, illustrating that the optimal number of latent variables for this PLS model was six.

An RGV of 0.45 was selected as a threshold value for bruising because most nonbruised images (50 × 50 pixels) had RGVs of >0.45 and most bruised images (50 × 50 pixels) had RGVs of <0.45. The RGVs in this experiment for pink salmon range from 0.24 to 0.69. The average RGVs for nonbruised and bruised tissue were 0.52 and 0.34, respectively. Approximately 84% of all nonbruised spectra were correctly classified, whereas approximately 81% of all bruised spectra were correctly classified. For instance, if the predicted RGV for a bruised

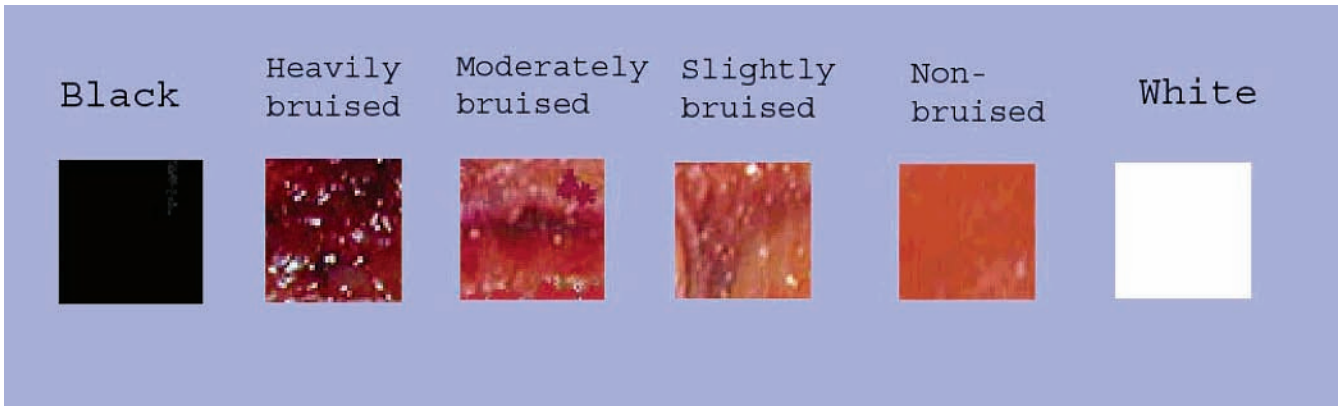

Figure 4. Digital images of different degrees of bruise in pink salmon muscle with black and white references (50 × 50 pixels).

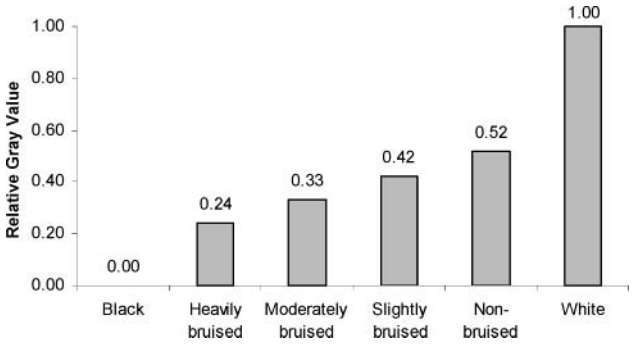

Figure 5. Mean relative gray value (RGV) of six digital images (50 × 50 pixels) in **Figure 4**.

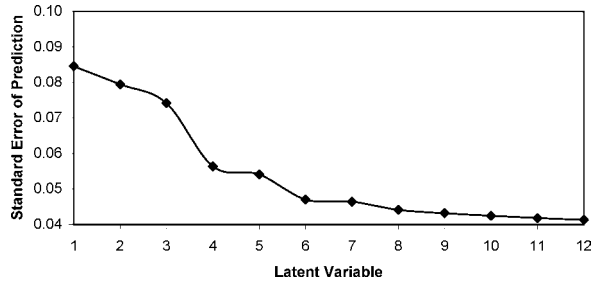

Figure 6. Standard error of prediction for PLS models for degree of bruising in pink salmon muscle.

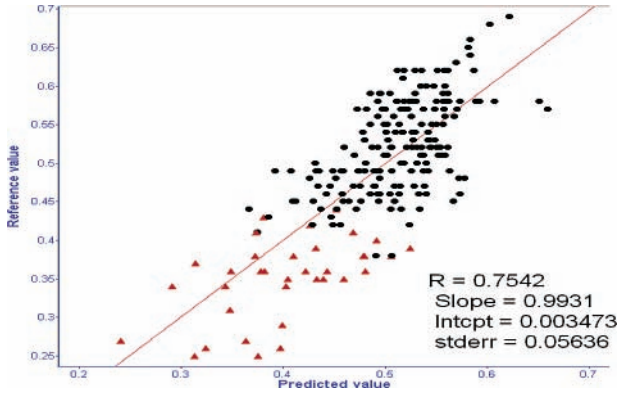

Figure 7. Comparison between the reference and predicted RGV for PLS model (four latent variables): (red triangles) spectra samples recorded on bruised locations; (black circles) spectra samples recorded on nonbruised locations.

spectral sample was below the cutoff point (0.45), the sample was correctly classified. On the contrary, if the predicted RGV was >0.45, the sample was wrongly classified. These results suggest that visible and SW-NIR could be used to detect and control the bruise defect of fish products during processing, therefore improving product consistency and quality.

Research with bruising in apples indicates that the effects of temporal factors, type of bruise, and severity of the bruise can affect infrared detection (750−1000 nm) (*5*). Lighting variations on the surface of the apples affected contrast between bruised and nonbruised regions. Others factors such as bruise type and bruise severity affected contrast and ability to detect these product defects (*5*). In our study, we observed that certain types of bruises, such as pooled blood near the tail region when the spine is fractured, were easier to detect than muscle contusions in thicker regions of the fish. Possibly some bruises may have been too deep to be detected with the small DPA-20 probe used in this study. Although light can penetrate 10 mm through fish skin, scales, and muscle with this probe, this may not have been

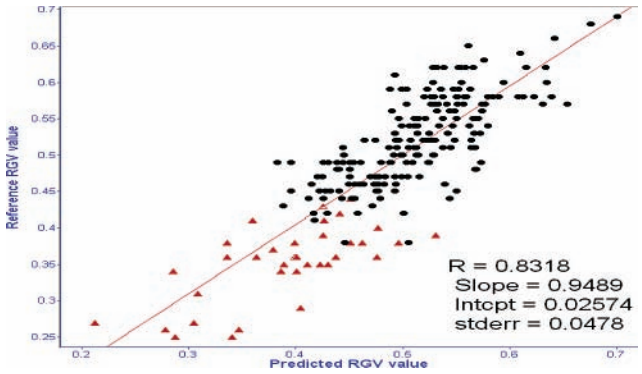

Figure 8. Comparison between the reference and predicted RGV for PLS model (six latent variables): (red triangles) spectra samples recorded on bruised locations; (black circles) spectra samples recorded on nonbruised locations.

sufficient to detect deeper muscle bruises (*12*). Better detection of muscle contusion should be possible if a large enough "signal" can be obtained from deeper tissue in the bruised area using a probe that emits a higher intensity light and which has a geometry permitting tissue illumination at greater penetration depth. Additional factors affecting the prediction results include the image resolution of the digital camera and the thickness of the fish skin and scales.

CONCLUSIONS

This study shows preliminary findings of the potential for using visible and SW-NIR spectroscopy (600−1100 nm) for noninvasively detecting the presence of bruises in the muscle of intact pink salmon. This technique could be of possible commercial relevance in aquatic industries and may be transferable to other food systems as well. Further studies are needed to confirm the feasibility of this technique in detecting bruises in other salmon species of greater commercial value such as coho, sockeye, and chinook, particularly for fish that are intended for smoked or cured preparations.

ACKNOWLEDGMENT

Special thanks are given to Dr. Quentin Fong, Dr. Charles Crapo (FITC), Dr. Jerry Babbitt (National Marine Fisheries Service), and Dr. Gleyn Bledsoe (Washington State University) for technical assistance with this project.

LITERATURE CITED

(1) Rasco, B. A.; Miller, C. E.; King, T. J. Utilization of NIR spectroscopy to estimate the proximate composition of trout muscle with minimal sample pretreatment. *J. Agric. Food Chem.* **1991**, *39*, 67−72.

(2) Pink, J.; Naczk, M.; Pink, D. Evaluation of the quality of frozen minced red hake: use of Fourier transform near-infrared spectroscopy. *J. Agric. Food Chem.* **1999**, *47*, 4280−4284.

(3) Huang, Y.; Tang J.; Swanson, B. G.; Cavinato, A. G.; Lin, M.; Rasco, B. A. Near infrared spectroscopy: a new tool for studying physical and chemical properties of polysaccharide gels. *Carbohydr. Polym.* **2003**, *53*, 281−288.

(4) Downey, G. Non-invasive and non-destructive percutaneous analysis of farmed salmon flesh by near infrared spectroscopy. *Food Chem.* **1996**, *55*, 305−311.

(5) Upchurch, B. L.; Throop, J. A.; Aneshansley, D. J. Influence of time, bruise-type, and severity on near-infrared reflectance from apple surfaces for automatic bruise detection. *Trans. ASAE* **1994**, *37*, 1571−1575.

(6) Agriculture and Agri-Food Canada. Fish and seafood on line. Wild Pacific salmon overview; 2003; http://atn-riae.agr.ca/seafood/pacific_salmon_overview-e.htm.
(7) Huang Y.; Rogers, T. M.; Wenz, M. A.; Cavinato, A. G.; Mayes, D. M.; Bledsoe, G. E.; Rasco, B. A. Detection of sodium chloride in cured salmon roe by SW-NIR spectroscopy. *J. Agric. Food Chem*. **2001**, *49*, 4161−4167.
(8) Huang, Y.; Cavinato, A. G.; Mayes, D. M.; Bledsoe, G. E.; Rasco, B. A. Non-destructive prediction of moisture and sodium chloride in cold smoked Atlantic salmon (*Salmo salar*). *J. Food Sci.* **2002**, *67*, 2543−2547.
(9) Rogers, T. M.; Cavinato, A. G.; Mayes, D. M.; Bledsoe, G. E.; Huang, Y.; Rasco, B. A. Nondestructive measurement of chloride and moisture in cured salmon roe by SW-NIR. *East. Oreg. Sci. J.* **1999**, *15*, 22−26.
(10) Clark, M. M.; Cavinato, A. G.; Mayes, D. M.; Rasco, B. A.; Sun, Y. Non-invasive SW-NIR spectroscopic method for the detection of lipid content in muscle of rainbow trout. *East. Oreg. Sci. J.* **1997**, *13*, 9−14.
(11) Lee, M. H.; Cavinato, A. G.; Mayes, D. M.; Rasco, B. A. Noninvasive short-wavelength near-infrared spectroscopic method to estimate the crude lipid content in the muscle of intact rainbow trout. *J. Agric. Food Chem*. **1992**, *40*, 2176−2181.
(12) Nord, S. P.; DuBreuil, R.; Cavinato, A. G.; Mayes, D. M.; Lin, M.; Rasco, B. A. Penetration depth studies in cod tissue using short-wave near-infrared spectroscopy. *East. Oreg. Sci. J.* **2001**−**2002**, 37.
(13) Rolfe, P. In vivo near-infrared spectroscopy. *Annu. Rev. Biomed. Eng.* **2000**, *2*, 715−754.
(14) Sigfusson, H.; Decker, E. A.; Morrissey M.; McClements, D. J. Ultrasonic characterization of north Pacific Albacore (*Thunnus alalunga*). *J. Aquat. Food Prod. Technol.* **2001**, *10* (3), 5−19.
(15) Peiris, K. H. S.; Dull, G. G.; Leffler, R. G.; Kays, S. J. Near-infrared (NIR) spectrometric technique for nondestructive determination of soluble solids content in processing tomatoes. *J. Am. Soc. Hortic. Sci.* **1998**, *123*, 1089−1093.
(16) Lin, M.; Cavinato, A. G.; Huang, Y.; Rasco, B. A. Predicting sodium chloride content in commercial king (*Oncorhynchus tshawytscha*) and chum (*O. keta*) hot smoked salmon fillet portions by short-wavelength near-infrared (SW-NIR) spectroscopy. *Food Res. Int.* **2003**, *36*, 761−766.
(17) Fennema, O. R. *Food Chemistry*, 3rd ed.; Dekker: New York, 1996.

Received for review June 10, 2003. Revised manuscript received August 17, 2003. Accepted August 19, 2003. This research was supported by the U.S. Department of Agriculture National Research Initiative Competitive Grants Program (NRICGP) Project 2000-01617 and Project 2000-01191, USDA Special Grant UAF 01-0048, the National Fisheries Institute, Eastern Oregon University, Textron Systems, and Washington State University.

JF0346197